Potential-Dependent Adsorption and Orientation of meso-Substituted Porphyrins at Liquid|Liquid Interfaces Studied by Polarization-Modulation Total Internal Reflection Fluorescence Spectroscopy

Supporting Information

Potential-Dependent Adsorption and Orientation of *meso*-Substituted Porphyrins at Liquid|Liquid Interfaces Studied by Polarization-Modulation Total Internal Reflection Fluorescence Spectroscopy

Sho Yamamoto,[†] Hirohisa Nagatani,*[,‡] Kotaro Morita[‡] and Hisanori Imura[‡]

[†] Division of Material Chemistry, Graduate School of Natural Science and Technology, Kanazawa University, Kakuma, Kanazawa 920-1192, Japan

[‡] Faculty of Chemistry, Institute of Science and Engineering, Kanazawa University, Kakuma, Kanazawa 920-1192, Japan

*To whom correspondence should be addressed: H. Nagatani

Tel: +81 76 264 5692; FAX: +81 76 264 6059; E-mail: nagatani@se.kanazawa-u.ac.jp

S1. Polarization modulation efficiency of the excitation beam.

The polarization modulation efficiency (P_m) of a liquid crystal retarder (LCR) in the present experimental setup was defined as the fraction of the p- or s-polarized component in the excitation beam through LCR. The intensities of p- and s-polarized incident beams, I^p and I^s, were measured by a Glan-Thompson prism (Sigma Koki, GTPC-10-33SN) and a Si photodiode (Hamamatsu Photonics, S1133-01) placed after LCR. As shown in **Figure S1**, the maximum I^p and I^s were observed under respective polarization conditions of LCR. The P_m values in the p- and s-polarized modes, P_m^p and P_m^s, are expressed by eqs. S1 and S2 under respective polarization modes, respectively.

$$P_m^p = \frac{I^p}{I^p + I^s} \qquad \text{(S1)}$$

$$P_m^s = \frac{I^s}{I^p + I^s} \qquad \text{(S2)}$$

The value of $P_m (= P_m^p = P_m^s)$ was obtained as 0.95 indicating that a 5% of the s-polarized component remains in the p-polarization mode of LCR or *vice versa*.

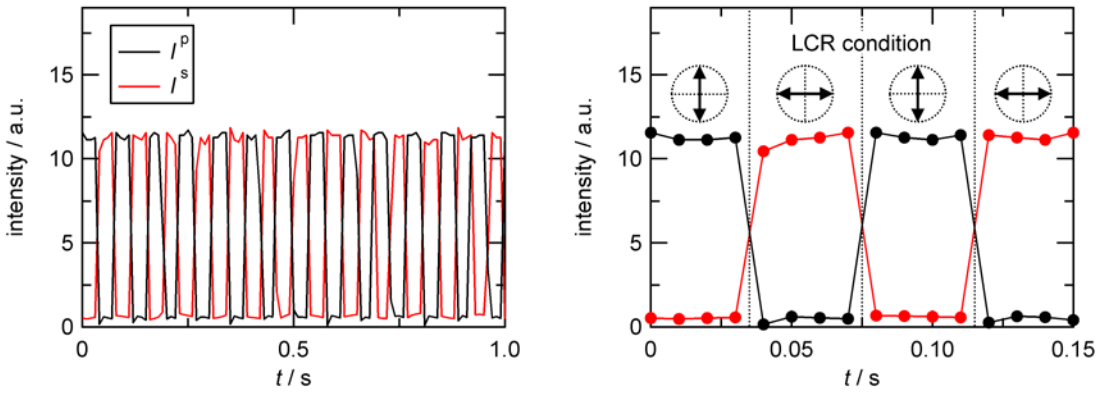

Figure S1. Typical time dependences of polarization-modulated light intensity through LCR at 13 Hz. The black and red lines refer to the intensities of the p- and s-polarized components of the excitation beam.

S2. Dependences of the fluorescence intensity on the linear polarization of excitation beam and molecular orientation

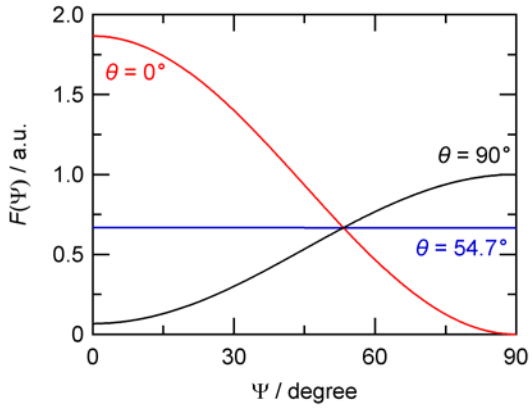

Figure S2. Polarization angle dependence of the fluorescence intensity ($F(\Psi)$) calculated from eq. 1. The angle of linear polarization of excitation beam (Ψ) was defined as the angle with respect to the interface normal, where 0° and 90° relate to the p- and s-polarization, respectively. The orientation angle (θ) was taken as 0°, 54.7° and 90°. The values of other parameters were taken as $C = 1$, $\alpha = 75°$, and $\theta = 0°, 54.7°, 90°$, respectively.

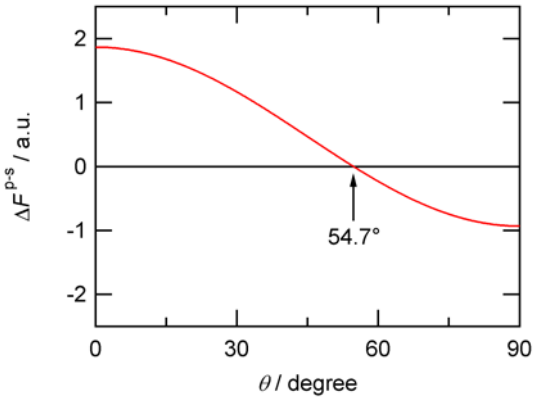

Figure S3. Orientation angle dependence of PM-TIRF signal ($\Delta F^{p\text{-}s}$) calculated from eqs. 1 and 5. The orientation angle (θ) of an adsorbed molecule was varied between 0° and 90°. The values of other parameters were taken as $C = 1$, $\alpha = 75°$ and $P_m = 1$, respectively.

S3. Ac voltammetric responses for ion transfer of H_2TMPyP^{4+} and H_2TPPS^{4-}

The ac voltammograms for H_2TMPyP^{4+} and H_2TPPS^{4-} at the water|DCE interface are shown in **Figure S4**. The well-defined ion transfer responses of H_2TMPyP^{4+} were obtained at around $\Delta_o^w\phi^{\circ'}_{H_2TMPyP^{4+}} = 0.07$ V (**Figure S4a**). On the other hand, a significant increase of the real (Y_{re}) and imaginary (Y_{im}) components of the admittance was measured in the H_2TPPS^{4-} system at potentials prior to the ion transfer potential, i.e. $\Delta_o^w\phi^{\circ'}_{H_2TPPS^{4-}} (= -0.20\text{ V}) < \Delta_o^w\phi$, which is associated with specific adsorption of H_2TPPS^{4-} at the interface (**Figure S4b**). These results indicate that H_2TPPS^{4-} is preferably adsorbed at the interface in comparison with H_2TMPyP^{4+}.[1,2]

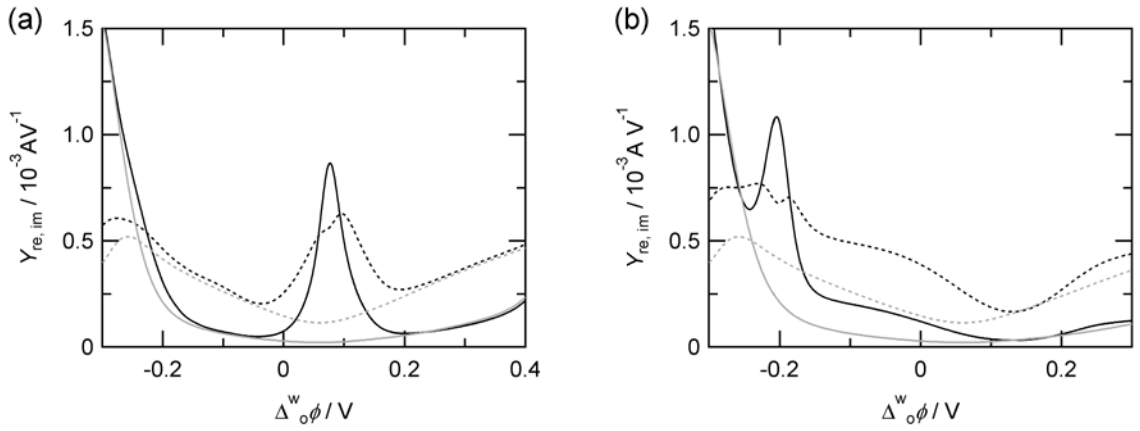

Figure S4. Real (solid line) and imaginary (dashed line) components of the admittance measured for (a) H_2TMPyP^{4+} and (b) H_2TPPS^{4-} at the water|DCE interface. The gray lines depict the admittances in the absence of the porphyrin. The potential modulation was 10 mV at 7 Hz.

S4. CVs and PM-TIRF responses for the simple transfer of tris(2,2′-bipyridine)ruthenium(II) ($Ru(bpy)_3^{2+}$) across the water|DCE interface

In order to clarify the surface sensitivity of the PM-TIRF technique, we applied the PM-TIRF spectroscopy to the tris(2,2′-bipyridine)ruthenium(II) ($Ru(bpy)_3^{2+}$) system. $Ru(bpy)_3^{2+}$ is an efficient fluorescent dye and it has been studied at the polarized water|DCE interface,[3,4] in which $Ru(bpy)_3^{2+}$ exhibited a quasi-reversible ion transfer feature without the interfacial adsorption. The formal transfer potential was observed as $\Delta_o^w\phi^{\circ'}_{Ru(bpy)_3^{2+}} = -0.10\,V$ in the voltammetric measurements (**Figure S5a**). A D_3 symmetry of $Ru(bpy)_3^{2+}$ ensures independence of the fluorescence intensity on linear polarizations of the excitation beam, even if $Ru(bpy)_3^{2+}$ is adsorbed at the interface. The $Ru(bpy)_3^{2+}$ system is therefore suitable to examine the selectivity of the PM-TIRF technique for the species "oriented" at the interface. As shown in **Figure S5b**, the PM-TIRF signals ($\Delta F^{p\text{-}s}$) were almost constant in the whole potential region and negligibly small in comparison with the total fluorescence intensity (F_{total}). In the absence of the interfacial adsorption, eq. (7) is simplified to $F_{total} = F_{bulk}$. Thus, F_{total} at $\Delta_o^w\phi < \Delta_o^w\phi^{\circ'}_{Ru(bpy)_3^{2+}}$ is identical to the

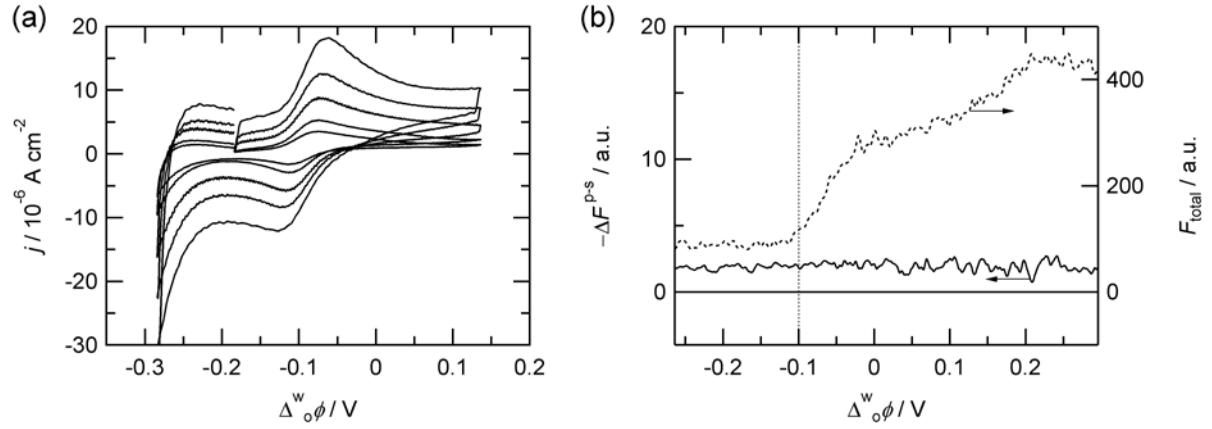

Figure S5. (a) Typical cyclic voltammograms and potential dependence of (b) PM-TIRF responses ($\Delta F^{p\text{-}s}$) measured for $Ru(bpy)_3^{2+}$ at the water|DCE interface. The potential sweep rates were (a) 10, 20, 50, 100 and 200 mV s^{-1}, (b) 5 mV s^{-1}. The concentration of $Ru(bpy)_3^{2+}$ derivatives in the aqueous phase was 2.0×10^{-5} mol dm^{-3}. The pH values of the aqueous phase were pH 7.0. The excitation and detected emission wavelengths were 404 nm and 609 nm, respectively. The vertical dotted line indicates $\Delta_o^w\phi^{\circ'}_{Ru(bpy)_3^{2+}} = -0.10\,V$.

fluorescence from the bulk aqueous phase and the significant increment of F_{total} at $\Delta^{\text{w}}_{\text{o}}\phi^{\circ'}_{\text{Ru(bpy)}_3^{2+}} < \Delta^{\text{w}}_{\text{o}}\phi$ associates with the fluorescence from Ru(bpy)_3^{2+} transferred into the organic phase. The potential dependence of F_{total} clearly showed that the fluorescence from the bulk organic phase effectively increases only at potentials beyond $\Delta^{\text{w}}_{\text{o}}\phi^{\circ'}$. It is noteworthy that $\Delta F^{\text{p-s}}$

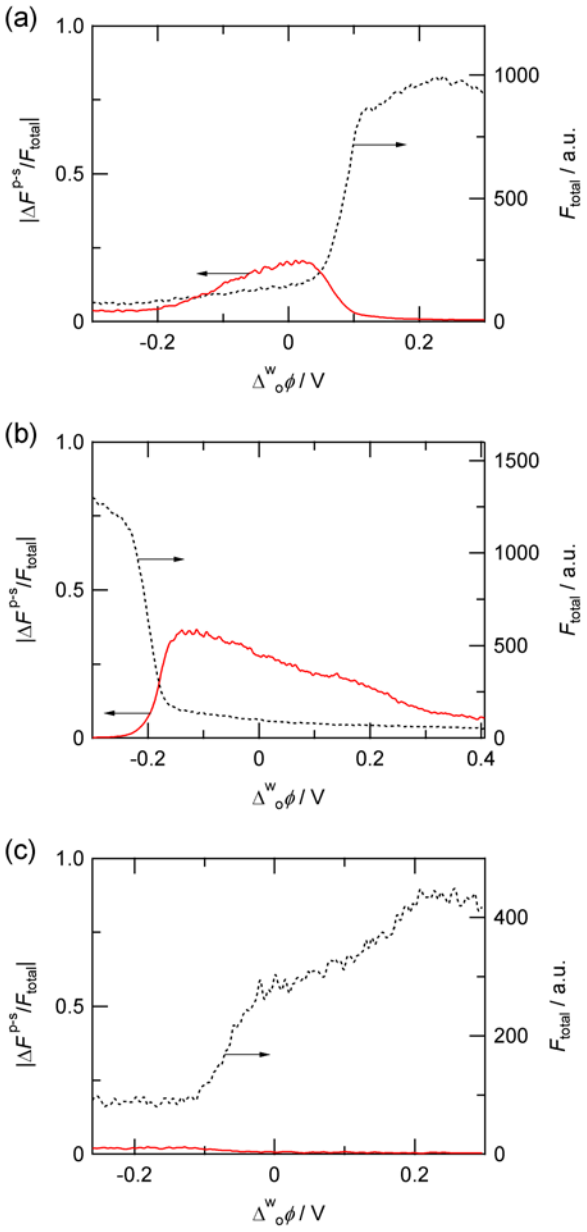

Figure S6. Potential dependences of $\left|\Delta F^{\text{p-s}} / F_{\text{total}}\right|$ for (a) H_2TMPyP^{4+}, (b) H_2TPPS^{4-} and (c) Ru(bpy)_3^{2+} systems. The dotted lines depict F_{total}.

was also independent on the F_{total} value consisting of the fluorescence intensities from both bulk solutions and interfacial region. **Figure S6** shows the relative intensity of $\Delta F^{\text{p-s}}$ with respect to F_{total}, $\left|\Delta F^{\text{p-s}} / F_{\text{total}}\right|$. The $\left|\Delta F^{\text{p-s}} / F_{\text{total}}\right|$ values observed for $Ru(bpy)_3^{2+}$ were much smaller than those for H_2TMPyP^{4+} or H_2TPPS^{4-}. These experimental results clearly demonstrate that only the species which have the excitation dipole moment oriented at the interface can generate strong PM-TIRF signals.

S5. PM-TIRF responses of H_2TMPyP^{4+} in the presence of Span 20

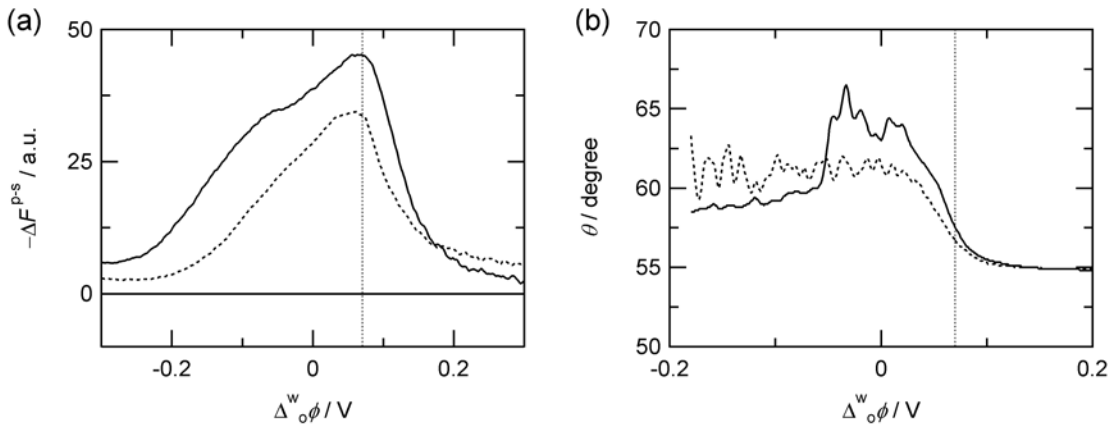

Figure S7. Potential dependences of (a) PM-TIRF ($\Delta F^{\text{p-s}}$) and (b) orientation angle (θ) estimated for H_2TMPyP^{4+} in the presence of Span 20. The solid and dashed lines relate to the H_2TMPyP^{4+} systems in the presence and absence of 1.0×10^{-3} mol dm^{-3} Span 20 in the organic phase. The excitation and detected emission wavelengths were 404 nm and 660 nm, respectively. The vertical dotted lines denote the ion transfer potential of H_2TMPyP^{4+} ($\Delta^{w}_{o}\phi^{o'}_{H_2TMPyP^{4+}} = 0.07$ V).

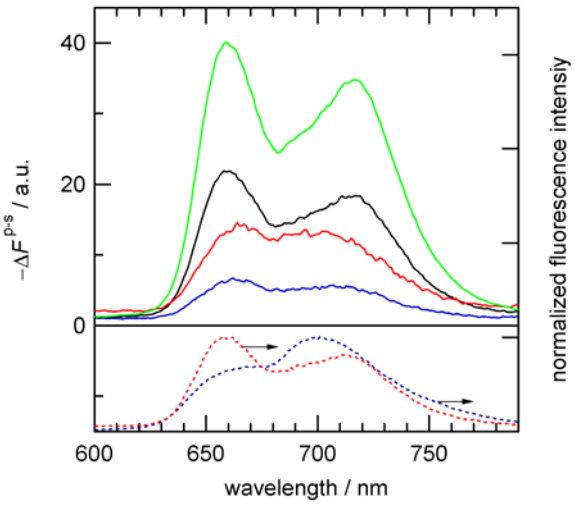

Figure S8. Potential dependent PM-TIRF spectra for H_2TMPyP^{4+} at the water|DCE interface in the presence of Span 20. The blue, black, green and red solid lines depict PM-TIRF spectra measured at −0.27 V, −0.15 V −0.06 V, and 0.19 V, respectively, in the presence of 1.0×10^{-3} mol dm^{-3} Span 20 in the organic phase. The blue and red dashed lines refer to normalized fluorescence spectra measured in the aqueous and organic solutions.

Table S1. Fluorescence maximum wavelengths (λ_{max}) of H_2TMPyP^{4+} at the water|DCE interface in the presence of Span 20 in the organic phase.

	H_2TMPyP^{4+} system		
	$\Delta_o^w\phi$ / V	λ_{max} / nm	R_F[a]
interface	0.19	663, 704	1.1
	−0.06	659, 715	1.2
	−0.15	660, 714	1.3
	−0.27	662, 708	1.2
aqueous phase[b]		660, 702	0.69
organic phase[b]		659, 712	1.2

[a]The peak intensity ratio of the first and second fluorescence peaks. [b]The fluorescence maximum wavelengths measured in the aqueous and organic solutions.

REFERENCES

(1) Nagatani, H.; Ozeki, T.; Osakai, T. *J. Electroanal. Chem.* **2006**, *588*, 99-105.

(2) Nagatani, H. In *Handbook of Porphyrin Science*, Kadish, K. M.; Smith, K. M.; Guilard, R., Eds.; World Scientific Publishing Co.: Singapore, 2014, pp 51-96.

(3) Ding, Z.; Wellington, R. G.; Brevet, P. F.; Girault, H. H. *J. Electroanal. Chem.* **1997**, *420*, 35-41.

(4) Nagatani, H.; Iglesias, R. A.; Fermín, D. J.; Brevet, P. F.; Girault, H. H. *J. Phys. Chem. B* **2000**, *104*, 6869-6876.